

Numerical and experimental study for the prediction of the steady, three dimensional flow in a turbine nozzle vane cascade using OpenFOAM

Silvia Ravelli*, Giovanna Barigozzi*, Francesco Pasqua**, Roberto Pieri[♦], Raffaele Ponzini**

*Department of Engineering and Applied Sciences, University of Bergamo, Dalmine (BG), Italy

**SCAI - SuperComputing Applications and Innovation – CINECA, Segrate (MI), Italy

[♦]SCS Italy, Segrate (MI), Italy

Email: silvia.ravelli@unibg.it, giovanna.barigozzi@unibg.it, f.pasqua@ceneca.it,
r.pieri@scsitaly.com, r.ponzini@ceneca.it

Web: www.unibg.it, www.hpc.cineca.it, www.scsitaly.com

Summary

This work reports the results of a cooperation between the Energy Systems and Turbomachinery (EST) Research Group at the Department of Engineering and Applied Sciences of Bergamo University, SCAI – CINECA and SCS Italy. The main goal is to explore the potential of the OpenFOAM Toolbox to study the flowfield in a high pressure turbine nozzle guide vane or, in other words, to characterize the turbine section of a gas turbine engine. The present study is the first step toward the introduction of the OpenFOAM software for such applications. The point is to exploit the joined perspectives of the High Performance Computing facilities available at CINECA and the license-free business model provided by OpenFOAM. The object of the investigation presented herein is a solid vane (uncooled) typical encountered in high pressure turbine stages, whose aerodynamic behavior has been characterized by EST Laboratory testing. The preliminary outcomes of the analysis at low speed are encouraging in terms of both accuracy with respect to experimental data and computational efficiency on HPC platforms.

Keywords

High pressure turbine vane, CFD modelling, OpenFOAM, aerodynamic performance

Vane geometry and numerical setup

The object of this investigation is a high loading profile typical of a first stage nozzle guide vane of a modern heavy duty GT. Details of the vane geometry are reported in Fig. 1. The vane profile is characterized by a pitch-to-chord ratio of $s/c = 1.04$ and an aspect ratio of $H/c = 0.69$. A design flow

turning of 70° is imposed. Since the aspect ratio is relatively low, secondary flows are expected to notably affect aerodynamic performance [1]. Nowadays, the detailed secondary flow pattern is well known. From the computational side, it has been established that inclusion of both inlet boundary layer and viscous effects at the endwall are necessary to obtain reasonable predictions. However, an accurate calculation of secondary flow losses may be difficult to achieve because of the limitations of transition and turbulence modelling [2].

One vane was included in the domain (Fig. 2): periodicity conditions were applied to simulate multiple vane passages in a linear arrangement. Only half of the real span was considered, with the symmetry boundary condition at midspan. The inlet of the passage was located $1.6 c_{ax}$ upstream of the vane leading edge, where the boundary layer behavior was available from experiments (Fig. 3). The outlet was located well downstream. The boundary conditions imposed the measured velocity profile of Fig. 3 at the inlet (*timeVaryingMappedFixedValue*) and static pressure at the outlet (*fixedValue* of $0 \text{ m}^2/\text{s}^2$) in order to simulate a low speed flow (exit isentropic Mach number of $M_{2is} = 0.2$), with low turbulence intensity.

In order to assess the grid sensitivity of the results presented, three hybrid grids were made in POINTWISE by Pointwise, Inc. 5 layers with structured hexahedra cells were attached to the vane walls while prism cells were used in the vane passage. A coarse grid consisting in 1.6 million cells was the base for progressive refining in the wake region and around the vane. The final hybrid mesh (Fig. 4) with 3.5 million cells was checked to be of good quality (maximum non orthogonality of about 37) and fine enough to assure grid independence. The average Yplus near the vane wall was about 36, so that the viscous sublayer is not resolved and wall functions can be applied instead.

Incompressible steady state RANS simulations were performed by using the *simpleFoam* solver. Two-equation turbulent models such as Standard k- ϵ , Realisable k- ϵ and the Shear Stress Transport (SST) k- ω were chosen to provide closure. In particular, the first model was used to carry out the grid sensitivity analysis. The last two models, which are commonly used in industrial turbomachinery applications, were applied to the final mesh to seek the most accurate prediction of aerodynamic performance. Experimental data available for validation consisted in the following:

- vane loading measured by means of instrumented vanes;
- midspan blade to blade flow measured by a 2D Laser Doppler Velocimetry system;
- total pressure distribution in wake region at midspan, at $X/c_{ax} = 1.50$;
- kinetic energy loss coefficient ζ distribution calculated from a 5-hole probe traversed along a plane at $X/c_{ax} = 1.53$.

For spatial discretization, the default *Gauss linear* option was chosen among the gradient schemes. Convection schemes were bounded, as typically done for steady-state solvers: *Gauss linearUpwind* was used for velocity whereas *Gauss upwind* was enough for turbulent quantities. As a scheme for all diffusion terms, *Gauss linear corrected* was used. At convergence, residuals were kept under 10^{-9} for all parameters. Moreover, velocity and pressure in the wake changed no more than 0.001% for at least 2000 iterations.

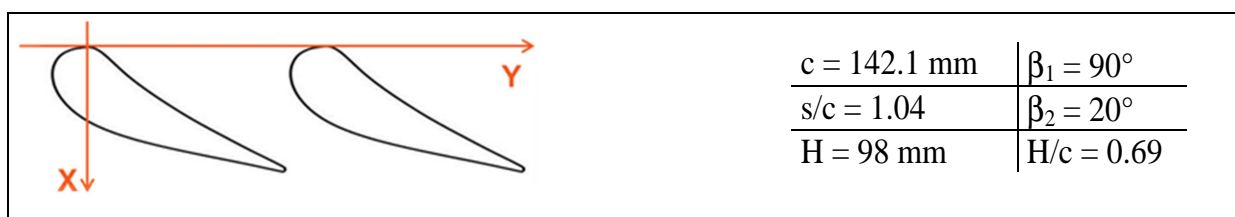


Figure 1: vane geometry

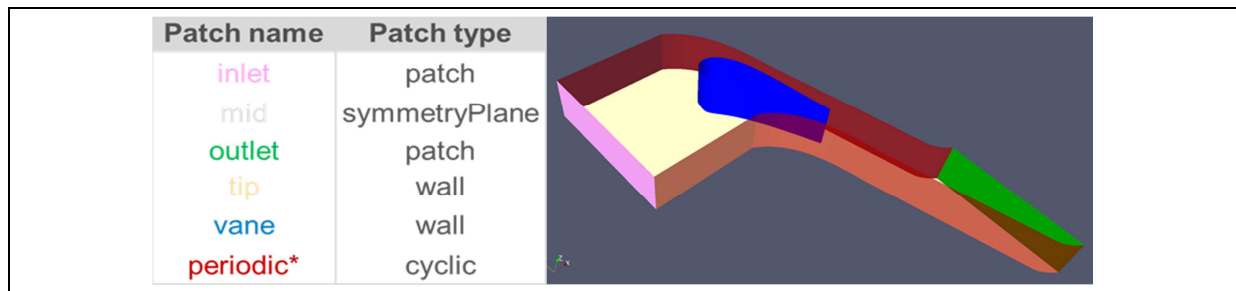


Figure 2: numerical domain

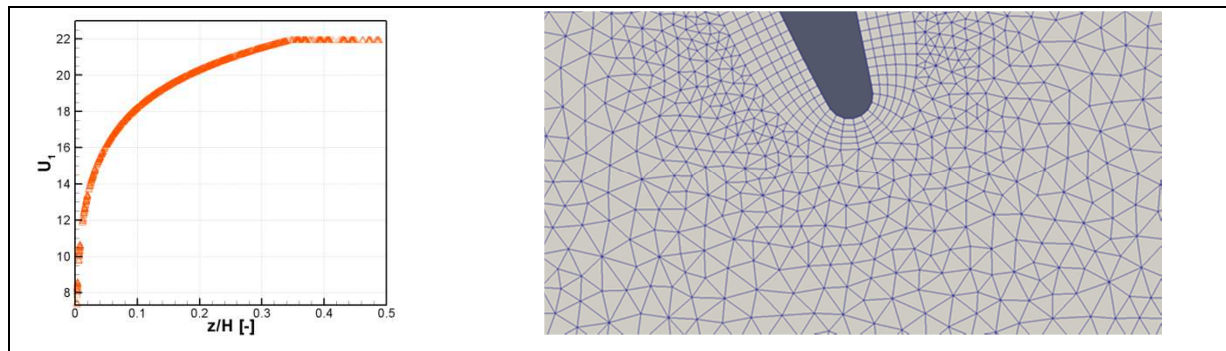
Figure 3: inlet boundary layer profile
($X/c_{ax} = -1.6$)

Figure 4: zoomed-in view of the final mesh

Results and discussion

Predictive capabilities of two-equation turbulence models in wide use today were assessed in comparison with detailed measurements of vane loading, blade to blade mid span velocity distribution, wake loss and secondary flow features. Results from the scalability analysis over different HW configurations were also discussed.

Midspan flow features

Experimental and numerical M_{is} profile distributions, normalized by the isentropic Mach number value at the trailing edge ($M_{is,TE}$), are shown in Fig. 5. Whatever the turbulence model, a satisfactory agreement between numerical and measured vane loading can be observed. In particular, the simulations captured pretty well the acceleration occurring along the vane pressure side up to the trailing edge. Also, predictions quite correctly reproduced the load profile along the suction side, even though a slight overestimation of the velocity maximum can be noticed between $0.1 c_{ax}$ and $0.4 c_{ax}$.

Fig. 6 illustrates the measured and the computed Mach number contours M in the mid span blade-to-blade plane. The M distributions look almost identical over the majority of the flow domain. Please note that only SST k- ω results are shown in Fig. 6 since midspan velocity predictions were found to have a weak dependence on turbulence model, as seen for the vane loading.

A direct comparison was also made between measured and calculated total pressure profile in the wake region, at $X/c_{ax} = 1.50$. A wake passage over one pitch is shown in Fig. 7. In general, the three simulations overestimated the wake loss, although to a different extent from case to case. In fact, the Standard k- ϵ provided the worst prediction whereas the best result was supplied by the SST k- ω . The latter overpredicted by about 9% the deficit in total pressure due to the wake. Actually, over-assessment of wake peak loss is typical for turbulence models assuming fully turbulent flows [3].

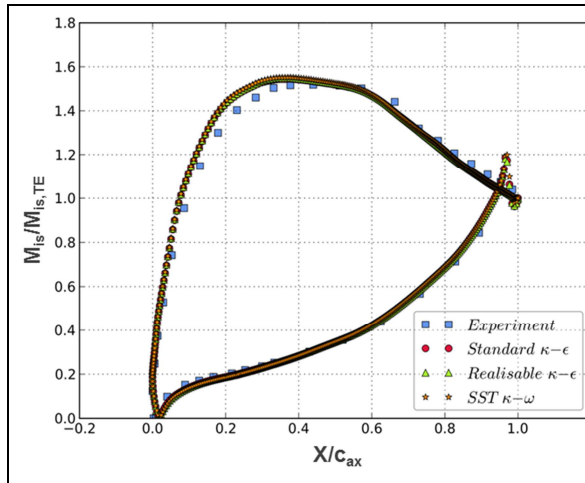


Figure 5: vane loading at midspan

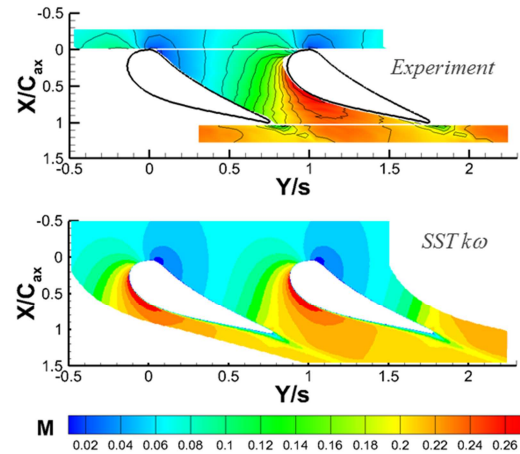
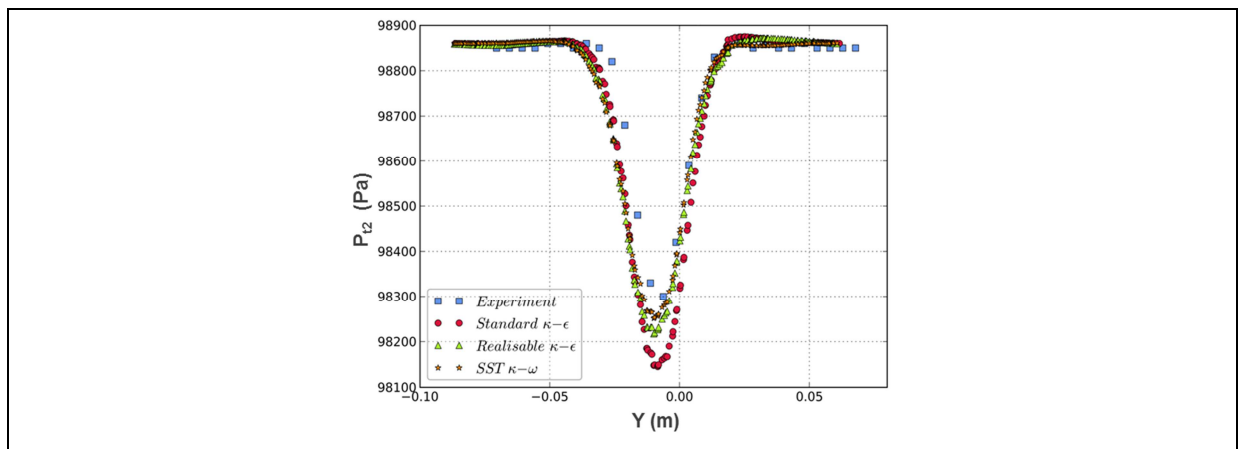


Figure 6: midspan blade-to-blade Mach number

Figure 7: total pressure loss profile at midspan ($X/c_{ax} = 1.50$)

Secondary flows

The most reliable turbulence model for wake predictions, i.e. SST k- ω , was further validated against experimental measurements of secondary flows, on a plane located at 53% c_{ax} downstream of the trailing edge (Fig. 8). The kinetic energy loss coefficient ζ was computed as follows:

$$\zeta = \left(1 - \frac{U_2^2}{U_{2is}^2} \right) * 100$$

With regard to measurements (left), most of the flow field is dominated by the passage vortex, as confirmed by the large, squeezed region of high losses on the suction side (SS) of the wake. The intensity and the extent of the passage vortex are related to aerodynamic load. In this case, the high pitch-to-chord ratio can be considered responsible for a quite intense passage vortex [4]. The loss peak associated with the corner vortex is higher than the one generated by the passage vortex. It can be observed that the wake is relatively thick and the 2D region is confined to a narrow span around the midspan (from about $Z/H = 0.3$ to 0.7).

From the comparison between experimental and numerical results, it emerged that the main vortical flow structures are correctly identified by SST k- ω turbulence model. However the kinetic energy losses associated with the passage vortex and the corner vortex are overestimated. Moreover, there are some differences in the shape of the secondary flow contours:

- the pitchwise distance between the computed loss cores of passage vortex and corner vortex is higher, with respect to measurements;
- the simulated corner vortex spreads over a greater pitchwise extent of the passage than that measured;
- the predicted passage vortex core is twisted towards the pressure side (PS) of the vane at about $Z/H = 0.8$, but this is not supported by experimental data.

Conversely, the SST $k-\omega$ model predicted the thickness of the wake reasonably well, coherently with the results of Fig. 7. The simulation also captured the loss core located in the wake within $0.4 < Z/H < 0.6$, even though its extension in the spanwise direction is slightly reduced, in comparison with measurements.

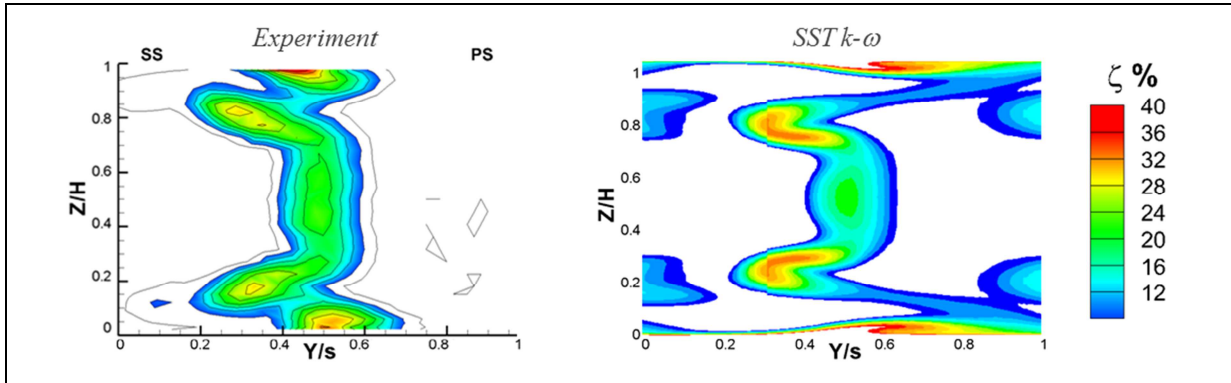


Figure 8: kinetic energy loss coefficient ζ distributions ($X/c_{ax} = 1.53$)

Scalability

The computational efficiency has been evaluated in order to take advantage of HPC platforms in an effective way. The case study has been run on three different hardware configurations in respect of both processors and interconnection. The number of computational cores used has been between 8 and 128, on a mesh with 3.5 million cells. The efficiency has been evaluated considering runs of 350 iterations from numerical convergence. The scalability curves are represented in Fig. 9.

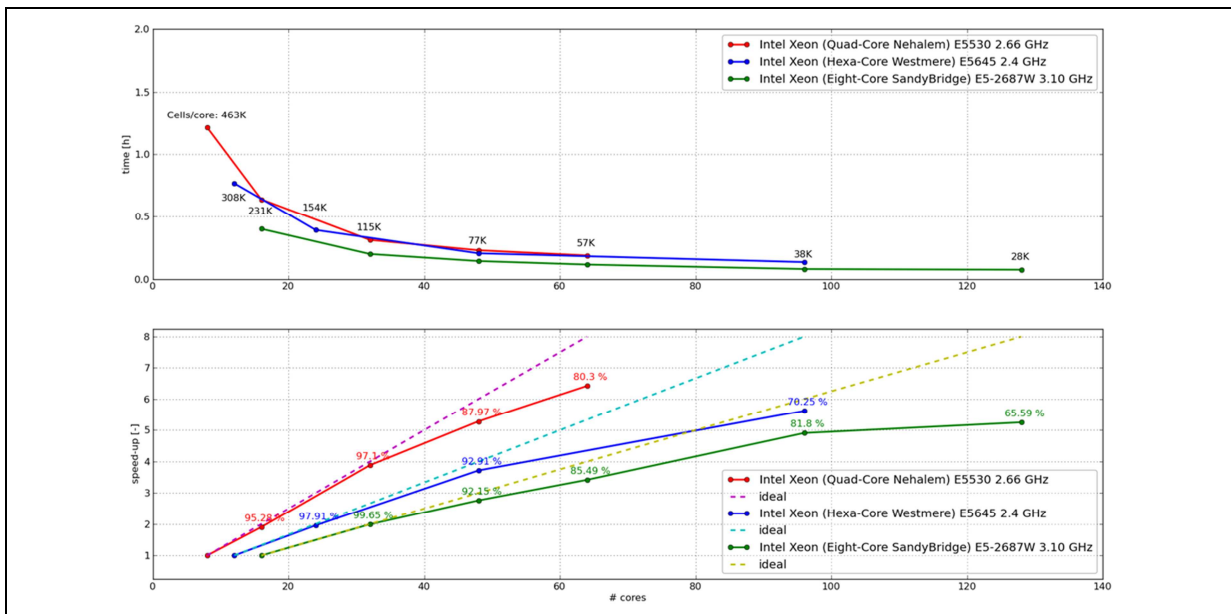


Figure 9: scalability

Conclusions

Aerodynamic measurements available from wind tunnel testing of uncooled, linear, nozzle vane cascade at low speed have been used to validate OpenFOAM predictions. Steady RANS equations were solved to compare the influence of different turbulence models in predicting vane loading, wake loss and secondary flow pattern. Standard and Realisable $k-\epsilon$, as well as SST $k-\omega$ models were considered in this study, thus revealing the following:

- vane load was predicted with satisfactory accuracy, especially on the pressure side, whatever the turbulence model.
- SST $k-\omega$ was the closest to the measured total pressure profile in the downstream flow, with an overestimation of the wake loss by about 9%.
- the secondary flow survey downstream of the vane confirmed that the SST $k-\omega$ model is able to provide reasonable predictions of the flow within the 2D wake region. On the opposite, kinetic energy losses associated with the highly 3-dimensional and vortical structures (passage and corner vortex flow) were overestimated.
- The scalability of this case study is effective on the tested cores range thanks to the HPC platform (HW + Interconnection).
- Setup showed a good efficiency (>80%) using up to 38k cells per computational core. This cell density per computational core can be used as reference for the same setup on larger problems.

References

- [1] Renaud E. W.: "Secondary Flow, Total Pressure Loss and the Effect of Circumferential Distortions in Axial Turbine Cascades", Massachusetts Institute of Technology, Department of Aeronautics and Astronautics, 1991.
- [2] Horloc J. H., Denton J.D.: "A Review of Some Early Design Practice Using Computational Fluid Dynamics and a Current Perspective", Journal of Turbomachinery, v. 127, January 2005, pp. 5-13.
- [3] Montis M., Niehuis R., M. Guidi, S. Salvadori, F. Martelli, B. Stephan.: "Experimental and Numerical Investigation of the Trailing Edge Bleeding on the Aerodynamics of a NGV cascade", paper n. GT2009-59910, From: ASME Turbo Expo 2009: Power for Land, Sea, and Air, v. 7: Turbomachinery, Parts A and B 2009, pp. 1063-1073.
- [4] Perdichizzi A., Dossena V.: "Incidence Angle and Pitch-Chord Effects on Secondary Flows Downstream of a Turbine Cascade", Journal of Turbomachinery, v. 115, July 1993, pp. 383-391.